J. Fluid Mech. (1977), *vol.* 80, *part* 2, *pp.* 237–257
Printed in Great Britain

Experiments on the fine structure of turbulence

By M. A. BADRI NARAYANAN, S. RAJAGOPALAN AND R. NARASIMHA

Department of Aeronautical Engineering, Indian Institute of Science, Bangalore 560012

(Received 29 October 1975)

Investigations have been carried out of some aspects of the fine-scale structure of turbulence in grid flows, in boundary layers in a zero pressure gradient and in a boundary layer in a strong favourable pressure gradient leading to relaminarization. Using a narrow-band filter with suitable mid-band frequencies, the properties of the fine-scale structure (appearing as high frequency pulses in the filtered signal) were analysed using the variable discriminator level technique employed earlier by Rao, Narasimha & Badri Narayanan (1971). It was found that, irrespective of the type of flow, the characteristic pulse frequency (say N_p) defined by Rao *et al.* was about 0·6 times the frequency of the zero crossings.

It was also found that, over the small range of Reynolds numbers tested, the ratio of the width of the fine-scale regions to the Kolmogorov scale increased linearly with Reynolds number in grid turbulence as well as in flat-plate boundary-layer flow. Nearly lognormal distributions were exhibited by this ratio as well as by the interval between successive zero crossings.

The values of N_p and of the zero-crossing rate were found to be nearly constant across the boundary layer, except towards its outer edge and very near the wall. In the zero-pressure-gradient boundary-layer flow, very near the wall the high frequency pulses were found to occur mostly when the longitudinal velocity fluctuation u was positive (i.e. above the mean), whereas in the outer part of the boundary layer the pulses more often occurred when u was negative. During acceleration this correlation between the fine-scale motion and the sign of u was less marked.

1. Introduction

It is now a well-established fact that the fine-scale structure of turbulence has some characteristic properties. As early as 1941, Kolmogorov postulated that at high Reynolds numbers the components of high frequency or small scale of any turbulent flow which is responsible for the dissipation of kinetic energy are in a certain type of universal equilibrium in which the dissipation rate ϵ and the kinematic viscosity ν are the only relevant parameters. Later, in 1949, Batchelor & Townsend observed that the high frequency part of the turbulence generated behind grids is intermittent and this observation suggested the possibility that turbulent motion is associated with a random distribution of concentrated

vorticity. This intermittent nature of turbulence was investigated by Sandborn (1959) in a general way and by Kennedy & Corrsin (1961) in shear flows and grid turbulence with special emphasis on the fine structure. Wyngaard & Tennekes (1970) extended the investigation to atmospheric turbulence, where the Reynolds numbers are high, and focused their attention mainly on the measurement of intermittency from the flatness factor. Detailed investigations of the fine structure of turbulence were carried out by Kuo & Corrsin (1971, 1972) by directly analysing filtered turbulent signals in grid and jet flows, which have shown many interesting features. Rao *et al.* (1971) studied the high frequency component of turbulence signals in boundary-layer flows and discovered that the appropriate scales were outer rather than inner variables. (The observations on 'bursts' reported by Rao *et al.* were based on measurements of the high frequency component of the turbulence signal. Since the same term is generally used to represent a whole cycle of phenomena near the wall (Kline *et al.* 1967), to avoid confusion we shall hereafter use the phrase 'high frequency pulses' to represent the observed high frequency activity in filtered turbulence signals.)

The geometry of the fine-scale regions has for some time been a matter of speculation. Originally it was proposed by Corrsin (1962) that these vorticity regions are sheet-like with thickness of the order of the Kolmogorov scale η and an average spacing of the order of the integral length scale L. It was shown by Tennekes (1968) that this model could not account for the total dissipation rate ϵ, and he suggested, on the basis of dimensional arguments, that these vortex regions should be tube-like instead of sheet-like, with diameter of the order of η and spacing of the order of the Taylor microscale λ. Experimental evidence of the tube-like nature of the fine-scale structure of turbulence is now available (Kuo & Corrsin 1972). However, on account of the highly idealized nature of the models and also owing to the indirect measurements used for guessing the shape, it is appropriate to consider the conclusions of Kuo & Corrsin to mean only that there is a marked tendency for the fine-scale regions to be predominantly filament-like in nature.

The separation of the fine-scale structure of turbulence for detailed study of its properties poses certain experimental difficulties, especially regarding the choice of the filter frequency. The investigations of Rao *et al.* have clearly indicated that the rate of occurrence N_p of the high frequency pulses in a turbulent flow increases linearly with the mid-band frequency f_m of the filter for low values of f_m but attains a constant asymptotic value at high f_m (figure 1). When conducted with a white-noise signal, the same experiment exhibited a linear variation of N_p with f_m throughout, without the kind of saturation in the value of N_p observed with the turbulence signal. An examination of the dissipation spectrum (Grant, Stewart & Moilliet 1962) indicates a maximum at about the Kolmogorov frequency

$$N_K \equiv \epsilon^{\frac{1}{4}}\nu^{-\frac{3}{4}}U/2\pi,$$

where U is the local mean velocity. The filter frequency at the beginning of saturation, say f_s, found in all experiments conducted in the present investigations happens to be about $\frac{1}{3}N_K$; frequencies beyond N_K make a negligible con-

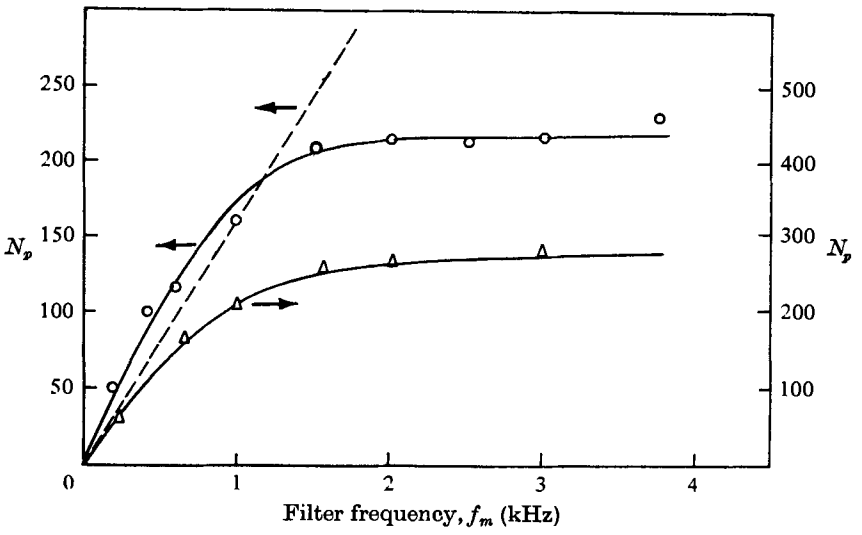

FIGURE 1. Variation of pulse rate with filter frequency. ——, f_s; – – –, white noise; ○, grid, $M = 1{\cdot}2$ in., $U = 30$ ft/s; △, flat plate, $R_\theta = 3000$, $y/\delta = 0{\cdot}4$.

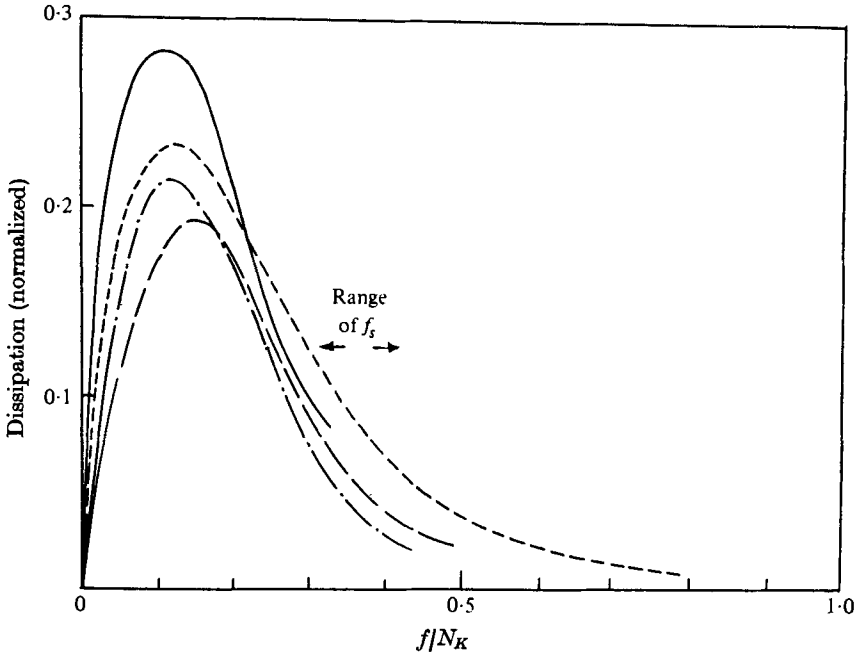

FIGURE 2. Dissipation spectra. ——, pipe; – – –, channel; —·—, boundary layer; ——, grid. N_K = Kolmogorov frequency. (For details see Grant *et al.* 1962.)

tribution to the dissipation (figure 2). Kuo & Corrsin (1971) have used N_K as the filtering frequency in their investigations whereas Rao *et al.* have employed f_s to separate out the high frequency components of the turbulence signals. Even though, according to the findings of Rao *et al.*, the filtering frequency does not affect N_p as long as it is beyond f_s, no investigations have been made so far on

the effects of the choice of filter frequency on the other characteristics of the high frequency pulses such as their width, internal structure, etc. We believe that f_s is the more appropriate frequency as it represents a characteristic saturation and is determined internally, and will therefore designate as 'fine-scale structure' the properties of signals filtered at f_s.

A brief account of the major findings of the investigations of Rao *et al.* is given below because of their relevance to the present work. In their boundary-layer measurements, the pulse rate N_p obtained using f_s as the mid-band filter frequency was such that the parameter $U_1/N_p\,\delta$ (where U_1 is the free-stream velocity and δ the boundary-layer thickness) was found to be practically independent of Reynolds number whereas the parameter $U_*^2/N_p\,\nu$, involving wall variables (namely ν and the friction velocity U_*), exhibited no such independence. The data on wall bursts obtained by Kline *et al.* agreed well with the data on the high frequency pulse rate of Rao *et al.* The above results led to the basic conclusion that the occurrence of the bursts could not be entirely a wall phenomenon, but must be triggered by other agencies. At that stage it was concluded that an interaction between the outer and inner flows was responsible for the turbulence production cycle. Measurements made in channel and wake flows exhibited similar results supporting the above view (Badri Narayanan, Rao & Narasimha 1971). However when the investigations were extended to grid flows (Badri Narayanan *et al.* 1971) to explore the generality of the phenomenon, no length scale producing Reynolds number independence could be found; in particular, the integral length scale L was not successful. Very recently this problem was examined further and the results reported in this paper are the outcome of this investigation. Experiments were carried out in grid turbulence as well as in boundary layers in zero and favourable pressure gradients. The high frequency pulses were always counted by the variable discriminator technique described by Rao *et al.*, and briefly outlined in the next section; the direct visual counting that was otherwise often used by Rao *et al.* was avoided to remove any personal judgement in the counting process.

Because preliminary results showed that the zero-crossing rate (say N_z) may be a significant variable, it was also measured in all the experiments. Liepmann, Laufer & Liepmann (1951) have shown that if turbulence were a Gaussian process we should have $N_z = U/\pi\lambda$; although this relation is nearly satisfied in grid turbulence, there appear to be deviations in shear flows. We therefore use

$$\Lambda \equiv U_c/\pi N_z \tag{1}$$

as an independent length scale, where U_c is an appropriate velocity; below we quote results adopting $U_c = U$ or U_1.

2. Experimental set-up

Experiments were conducted (i) in grid turbulence, (ii) in constant-pressure boundary-layer flow and (iii) in a reverting boundary layer subjected to a large favourable pressure gradient. The grid-turbulence and flat-plate measurements were conducted in a 20×20 in. wind tunnel, and the accelerated-boundary-layer

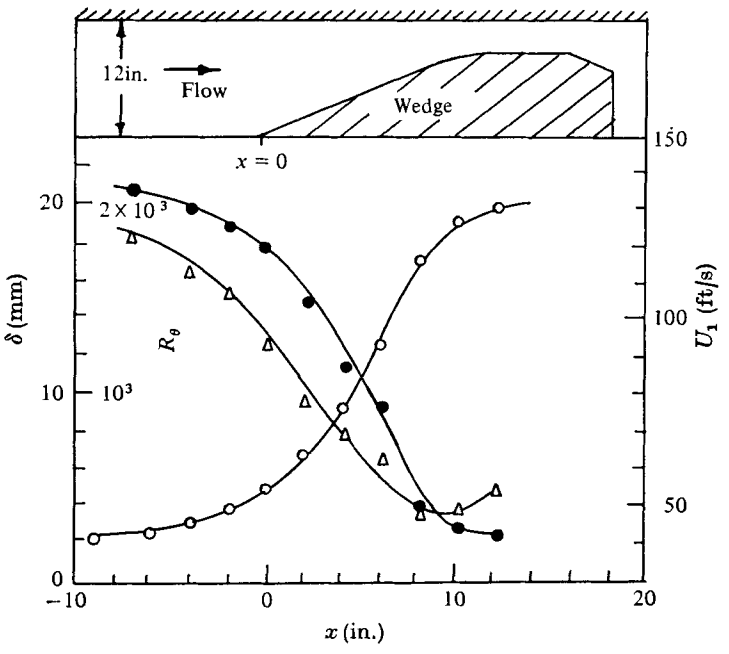

FIGURE 3. Variation of free-stream velocity and boundary-layer parameters during acceleration. ○, U_1; ●, δ; △, R_θ.

experiments in a 1 × 1 ft wind tunnel. In the grid experiments, the following three grids were employed:

mesh size (in.):	1·2,	0·5,	0·25;
wire diameter (in.):	0·19,	0·07,	0·04.

All measurements were made 90 in. downstream of the grids. Three flow velocities of about 30 ft/s, 40 ft/s and 60 ft/s were used, which resulted in a set of nine grid–velocity combinations. The grid measurements consisted of the r.m.s. value u' of the longitudinal velocity fluctuation, the dissipation

$$\epsilon = 15\nu \overline{\left(\frac{\partial u}{\partial t}\right)^2} / U^2,$$

and the rate N_z of zero crossings of the fluctuating u signal. High frequency pulses were recorded in all nine grid flows.

The zero-pressure-gradient measurements were conducted on the smooth, highly polished surface of the top wall of the wind tunnel. Suitable trips of rough emery paper (grade 36) were glued to the beginning of the test section to fix transition and to obtain a fully developed two-dimensional turbulent boundary layer at the measurement station 90 in. downstream. By varying the tunnel speed, the Reynolds number R_θ, based on free-stream velocity and momentum thickness, could be varied over the range 1900–5500. The measurements in the zero-pressure-gradient boundary-layer flows consisted of profiles of mean and turbulent velocity U and u, the dissipation ϵ, the rate N_z of zero crossings and the rate N_p of high frequency pulses. In addition the Reynolds-stress contributions

from each of the four quadrants, namely $\overline{u_+v_+}$, $\overline{u_-v_-}$, $\overline{u_-v_+}$ and $\overline{u_+v_-}$, were measured at $R_\theta = 3000$. (Here the subscripts $\pm$ denote the sign of the velocity fluctuation.) The experiments were carried out at six different Reynolds numbers: $R_\theta = 5500$, 4800, 4200, 3500, 3000 and 1900.

A 40° two-dimensional wedge on the floor of the 1 × 1 ft wind tunnel was used to produce an accelerated layer on the top wall (figure 3). Only one set of experiments was performed, under conditions corresponding roughly to an experiment conducted earlier in the same wind tunnel by Badri Narayanan & Ramjee (1969, experiment 4). The measurements consisted of profiles of mean velocity, u' and v', the Reynolds stress $-\overline{uv}$, the dissipation ϵ, the zero crossings of the u signal and the high frequency pulses.

For mean velocity measurements a Pitot tube with a 0·015 in. opening was employed. Static pressure holes of diameter 0·5 mm were drilled on the top wall at convenient distances along the centre-line and pressures were measured to an accuracy of 0·1 mm of alcohol. Both constant-current and constant-temperature hot-wire anemometers were used. They were built locally and had a flat frequency response from 2 Hz to 10 kHz. Both the single-wire and the cross-wire probes consisted of Pt–Rh wires 0·0002 in. in diameter and each 1 mm long. Great care was taken to align the cross-wires perpendicular to each other and also to ensure that there was a negligible difference in resistance (less than 2 %) between them. A solid-state electronic differentiator was used for measuring $\overline{(\partial u/\partial t)^2}$.

3. Method adopted for counting high frequency pulses and zero crossings

The high frequency pulses were separated from the u signal using a Krohn–Hite filter (Model 3550R), which was always set for a bandwidth of 0·2 times the centre-frequency. A splitter circuit was devised which separated the turbulent signals into positive and negative fluctuations from the mean. This circuit was employed in conjunction with a multiplier and an integrator circuit to separate out the contributions from the four quadrants of the u, v plane to the Reynolds stress $-\overline{uv}$. The high frequency pulses as well as the split signals were recorded on 35 mm film using a continuous drum-type camera at film speeds of about 7 ft/s.

The criterion for selecting the filter frequency for separating the high frequency pulses has already been described in the previous section. The method used for estimating N_p is essentially that described by Rao *et al.* and is briefly as follows (also see figure 4).

(*a*) On a projection of the photographic record of the filtered signal, an envelope with a hold time equal to $1/f_s$ is drawn.

(*b*) The number of pulses per unit time, say N, is counted (manually) using various discriminator settings D on the recorded trace.

(*c*) The number N is plotted against D.

(*d*) The maximum value of N on this curve is taken as N_p.

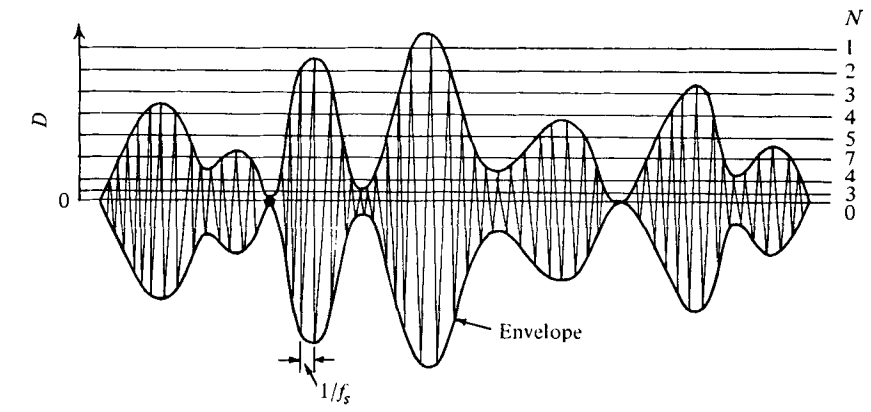

Trace of filtered signal

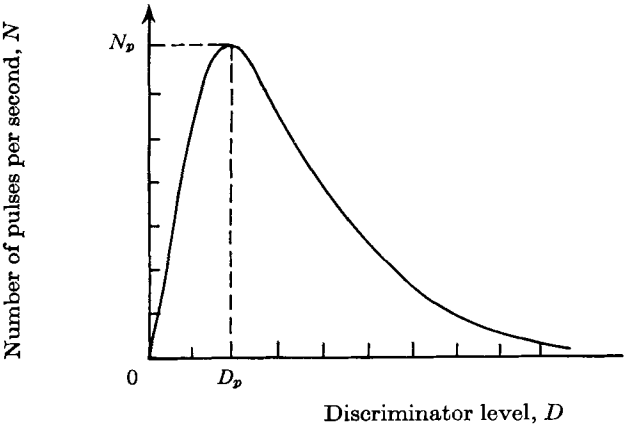

FIGURE 4. Method used for the determination of the high frequency pulse rates.

The discriminator level D_p corresponding to N_p is also taken as the reference level at which the width of the pulses is measured.

The following method is adopted for estimating the zero-crossing rate N_z. The output of the splitter circuit divides the u signal into sections in which the fluctuation in u from the mean value is positive or negative; each section is termed a run. Since a positive run is always followed by a negative run and vice versa, the number of zero crossings is twice the number of runs, which is again counted from a photographic record of the split signal. The length of a run (positive or negative) is always measured along the mean line between the two consecutive zero crossings corresponding to that particular run. $N_r = \frac{1}{2}N_z$, where N_r is the frequency of the runs.

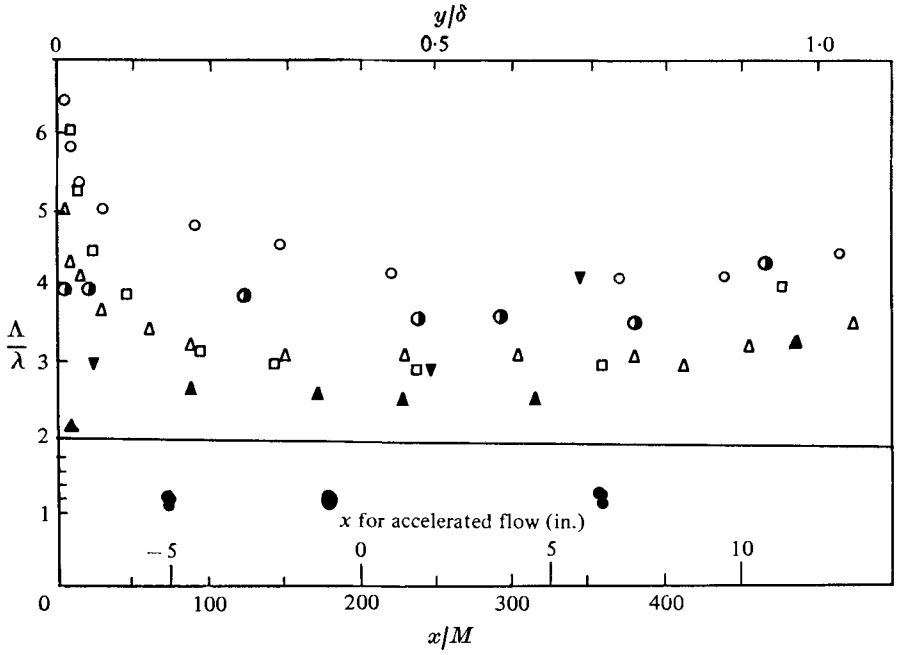

FIGURE 5. Ratio of zero-crossing length scale to Taylor microscale. Flat plate: ◑, ○, $R_\theta = 4800$; ▲, △, $R_\theta = 3000$; □, $R_\theta = 1860$. ●, grid; ▼, accelerated flow. ◑, ▲, Λ estimated using U; other symbols, Λ estimated using U_1.

4. Experimental results

The experiments in grid turbulence were made in the Reynolds number range $R_\lambda \equiv u'\lambda/\nu = 15$–$65$. The value of λ was estimated in the usual way from the time-derivative measurements using the relation

$$\lambda^2 = U^2 u'^2 \Big/ \overline{\left(\frac{\partial u}{\partial t}\right)^2}.$$

The flat-plate boundary layer exhibited the appropriate logarithmic region and velocity defects as defined by Coles (1962) at all six Reynolds numbers tested. Although these Reynolds numbers are not very high, and it may appear possible that interfacial intermittency from the outer edge may penetrate close to the surface, it is believed that the final results have not been severely affected by this, especially as no strong Reynolds number effects were found. The measurements of u', the Reynolds stress $-\overline{uv}$ and the dissipation agree fairly well with those of Klebanoff (1954), indicating that the boundary layers are not only fully developed but also of the standard form. The zero-crossing length scales were estimated in all the flows from the measured zero-crossing rate using (1). The ratio of the two length scales Λ/λ is shown in figure 5 for grid turbulence and flat-plate boundary-layer flow, using $U_c = U$ or U_1 in (1). Some points for the accelerated flow are also shown for comparison. In grid turbulence (where $U = U_1$) the ratio Λ/λ is nearly equal to 1·2, a result which is in conformity with those reported by Liepmann *et al.* (1951).

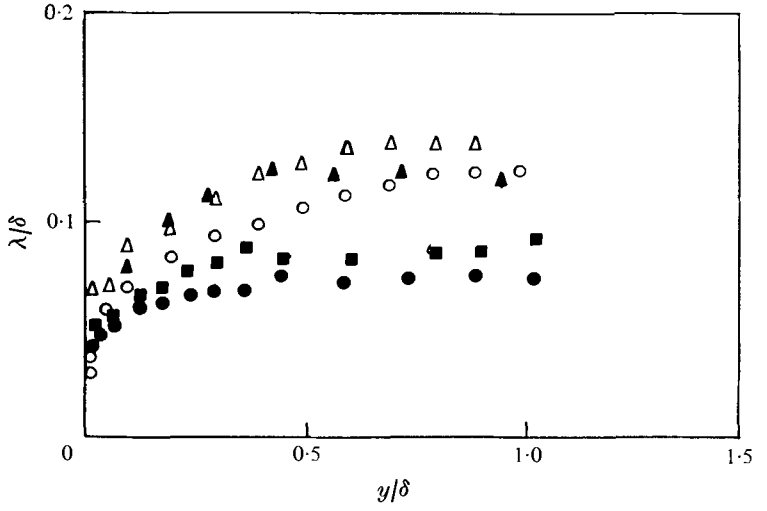

FIGURE 6. Distribution of Taylor microscale across the boundary layer for flat-plate flow. ○, Blackwelder & Kovasznay (1970), $R_\theta = 2950$, $R_\delta = 28000$; ■, present results, $R_\theta = 3000$, $R_\delta = 24000$; ●, present results, $R_\theta = 48000$, $R_\delta = 44000$; ▲, present results, $R_\theta = 1860$, $R_\delta = 17000$; △, Antonia (1973), $R_\theta = 1800$, $R_\delta = 18000$.

Figure 5 shows that using either U or U_1 the value of Λ/λ is appreciably different from unity at all three Reynolds numbers ($R_\theta = 1860$, 3000, 4500). Although U is the more common choice (and is compulsory if Taylor's hypothesis is adopted), the striking constancy of N_z across the boundary layer shown in figure 7 suggests that a constant velocity (like U_1) is equally if not more appropriate.

These relatively large values of Λ/λ were unexpected; to check them the values of dissipation measured in the flat-plate boundary layers were again checked with the standard values of Klebanoff and good agreement (within 5 %) was found at all three Reynolds numbers (for details see Badri Narayanan, Rajagopalan & Narasimha 1974). Comparison of the present values of the Taylor microscale λ with the available data of others (figure 6) shows good agreement, indicating that the present estimates of λ are not unusual. Finally, experiments in the two different wind tunnels mentioned earlier yielded the same conclusion.

The values of Λ/λ in a favourable-pressure-gradient boundary layer (figure 5) show a trend similar to that in a zero pressure gradient. These differences in the values of Λ/λ between grid and boundary-layer flows must presumably be attributed to the non-Gaussian nature of the turbulence signals in the latter flow.

The rate of occurrence N_p of the high frequency pulses was counted for all the cases by filtering the u signal using f_s as the filter frequency and employing the discriminator setting techniques described earlier. The measured values of N_p varied by a factor of two in grid turbulence over the Reynolds number range covered, and by a factor of three in boundary layers. N_p was found to be constant all across the flat-plate boundary layer except very near the wall and the outer edge, where a slight reduction was noticed. This trend was observed in the case of the accelerated boundary layer also, indicating that it is a common feature

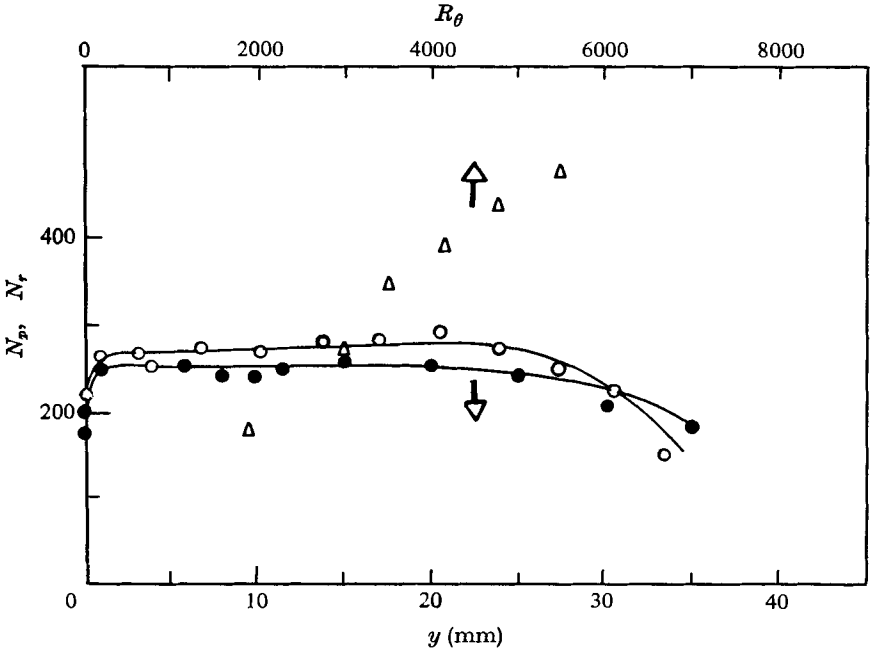

FIGURE 7. Distribution of pulse and run rates across the boundary layer for flat-plate flow at $R_\theta = 3000$. ○, pulses; ●, runs; △, N_p at $y/\delta = 0{\cdot}4$. $N_r = \frac{1}{2}N_p$.

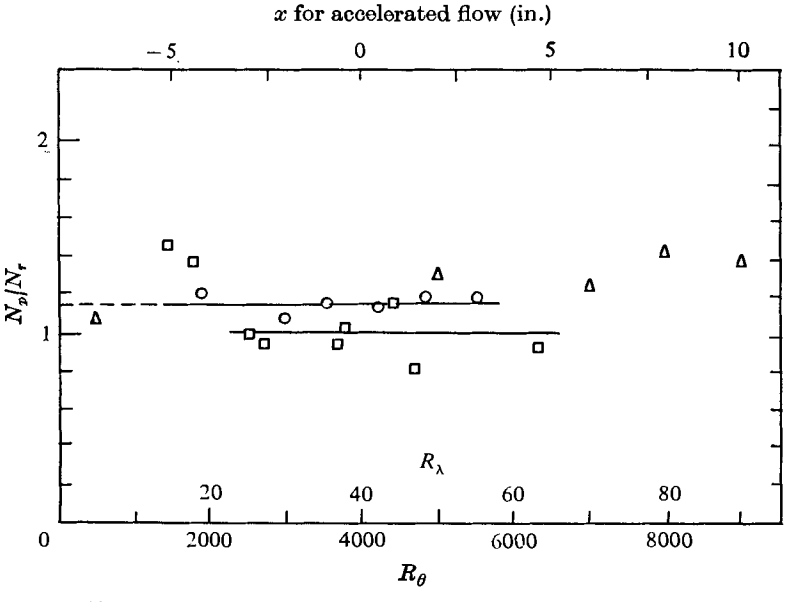

FIGURE 8. Ratio of pulse rate to run rate. ○, flat-plate flow, $y/\delta = 0{\cdot}4$; △, accelerated flow, $y/\delta = 0{\cdot}5$; □, grid flow.

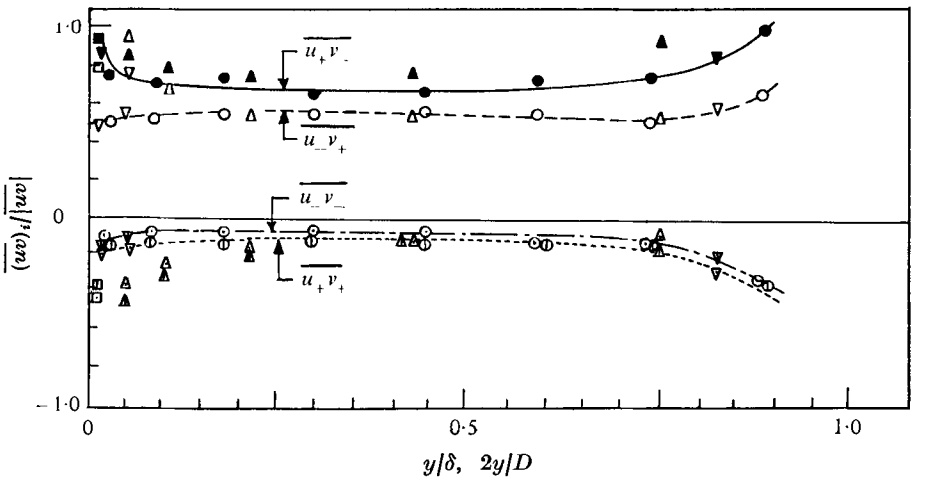

FIGURE 9. Contribution to Reynolds stress from the four quadrants. D = full width of channel. ▽, Lu & Willmarth (1973), boundary layer; △, Brodkey *et al.* (1974), channel; ○, present measurements, boundary layer.

of any boundary-layer flow. The zero-crossing rate N_z shows the same trend as the frequency of pulses. The variation of N_p and N_z across a flat-plate boundary layer at a Reynolds number of 3000 is shown in figure 7. It is interesting to note that N_z is very nearly twice N_p. Also shown in this figure is the variation of N_p with an appropriate Reynolds number for all three different flows. It is seen (figure 5) that the ratio N_p/N_z is nearly 0·6 irrespective of the type of flow.

In flat-plate boundary layers, the contributions from the four different quadrants to the Reynolds stress were measured at a Reynolds number of 3000 (figure 9). For comparison, the measurements made by Lu & Willmarth (1973) in a boundary layer and by Brodkey, Wallace & Eckelmann (1974) in a two-dimensional channel are also plotted in the same figure. There is reasonable agreement among all the results.

Oscilloscope traces of the high frequency pulses and the split turbulence signal, when viewed simultaneously, showed some interesting trends. Very close to the wall ($y/\delta < 0{\cdot}02$), the high frequency pulses tended to occur† during positive runs of the u signal. This trend exists up to $y_* = 20$; beyond this region no significant synchronization could be detected. When the hot-wire probe was moved towards the outer edge of the boundary layer, there was again synchronization but with the negative part of the u signal and the positive part of the v signal. No v measurements could be made very close to the wall owing to the size of the cross-wire probe. To illustrate these observations in a quantitative way, we define a *coincidence coefficient*, which is the average number of runs in which pulses occur entirely within the particular type of run, as a fraction of the total. Figure 10 shows the results of the present measurements. It is seen that the sum of the coincidence coefficients for positive and negative runs

† In a preliminary account of this work (Badri Narayanan *et al.* 1974) there was an unfortunate typographical error in the sign of u for the runs for which the coincidence coefficients were quoted.

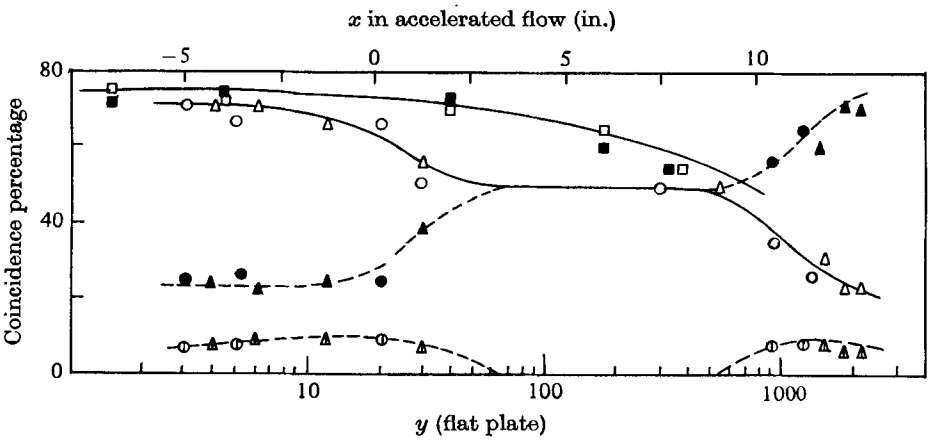

FIGURE 10. Degree of coincidence between high frequency pulses and runs. Open symbols, u_+ and pulse; filled symbols, u_- and pulse; divided symbols, overlap. Flat-plate flow: △, $R_\theta = 5500$, ○, $R_\theta = 3000$. Accelerated flow: ■, $y = 0{\cdot}05$ mm; □, $y/\delta = 0{\cdot}9$.

respectively is slightly less than unity, because of cases of 'overlap' in which the pulse was not confined to a single positive or negative run. The percentage of overlap is seen to be quite small. Similar experiments were carried out in accelerated flows and the results are shown in the same figure. These measurements were made at $y/\delta = 0{\cdot}9$. In the accelerated flow, the coincidence drops slowly from nearly 80 % before acceleration to 50 % at the end.

5. Discussion

The major aim of the present investigation is to examine the length scales associated with the fine-scale regions of turbulence with special emphasis on the average spacing between them and their width. Since the experiments of Kuo & Corrsin (1972) have already indicated, though indirectly, that the vorticity regions are tube or filament like, the 'width' of the vortex tubes denotes their average diameter. If one assumes that the vortex tubes, which are randomly oriented in the flow, are convected at nearly the free-stream velocity U_1, then the average distance between neighbouring tubes is U_1/N_p. As the vortex geometry is governed by some characteristics of the flow, it is reasonable to presume that U_1/N_p should scale with some length associated with the flow irrespective of the flow Reynolds number (provided that this is sufficiently high).

In grid turbulence, as has already been pointed out, the integral length scale L has been found to be inappropriate. In the present investigation three other length scales, namely the grid mesh size M, the Taylor microscale λ and the zero-crossing length scale Λ, were tried with the results shown in figures 11 and 12. The non-dimensional parameters $U_1/N_p M$ and $U_1/N_p L$ indicate a strong dependence on the Reynolds number R_λ. Only $U/N_p \Lambda$, which in grid turbulence is almost equal to $U/N_p \lambda$, is nearly constant over the Reynolds number range covered in the present experiments, with a value of around 6·0. The integral length scale L was not measured in the present experiments, but estimated from

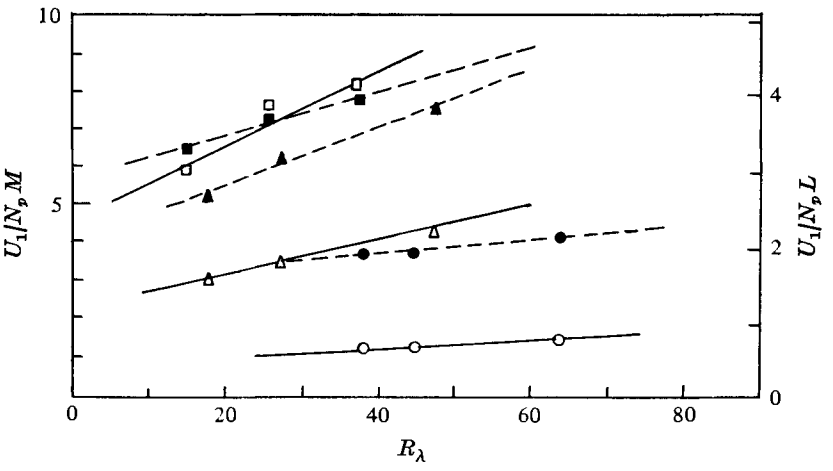

FIGURE 11. Scaling of pulse rate with mesh size and integral length scale. Grid flow, $x = 90$ in. M (in.): ●, ○, 1·20; ▲, △, 0·50; ■, □, 0·25. – – –, $U_1/N_p L$; ——, $U_1/N_p M$.

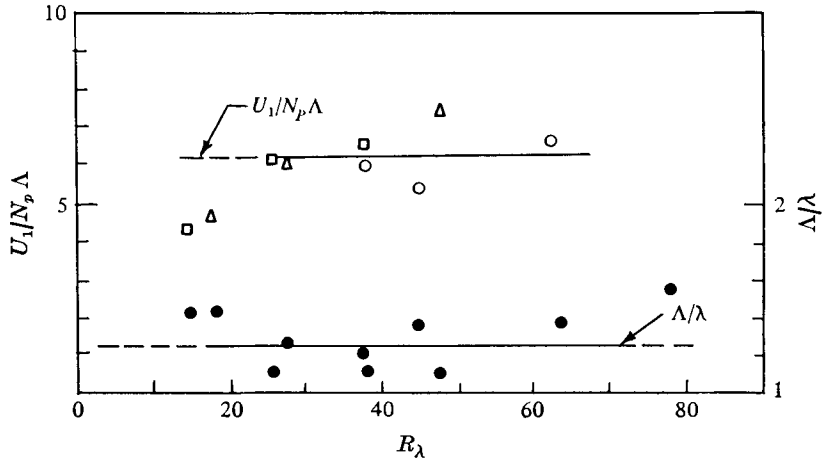

FIGURE 12. Scaling of pulse rate with zero-crossing length scale and the ratio of the Taylor microscale to the zero-crossing length scale. M (in.): ○, 1·20; △, 0·50; □, 0·25.

the already available data shown as $(L/M)^2$ *vs.* x/M by Batchelor & Townsend (1948). The values of L thus estimated were also examined for their reliability by plotting R_λ *vs.* $R_L^{\frac{1}{2}}$. This plot indicated a good linear relationship. These results clearly indicate that neither the integral scale L nor the grid mesh size M is the appropriate length scale. The microscale λ and the zero-crossing length scale seem to be the relevant ones and this result is in conformity with the argument of Tennekes (1968).

Similar non-dimensionalization with various length scales in boundary-layer flows indicated somewhat different trends. The length scales employed were δ, λ and Λ. Since N_p varies negligibly with y over most of the boundary layer, the results are plotted for comparison at a distance $y/\delta = 0{\cdot}4$ (figure 13). The non-dimensional parameters $U_1/N_p\,\delta$, $U_1/N_p\,\lambda$ and $U_1/N_p\,\Lambda$ are all nearly independent of

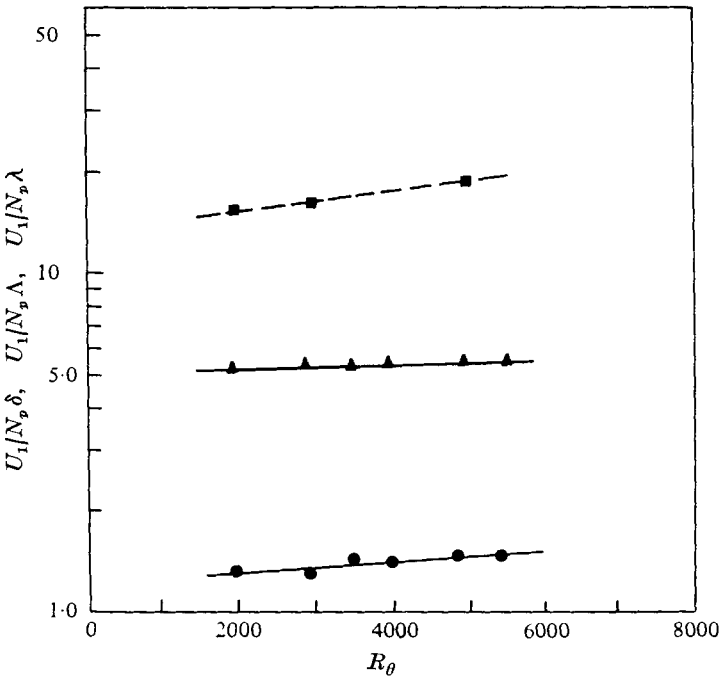

FIGURE 13. Scaling of pulse rate with various length scales. Flat plate, $y/\delta = 0{\cdot}4$. ●, $U_1/N_p\delta$; ▲, $U_1/N_p\Lambda$; ■, $U_1/N_p\lambda$.

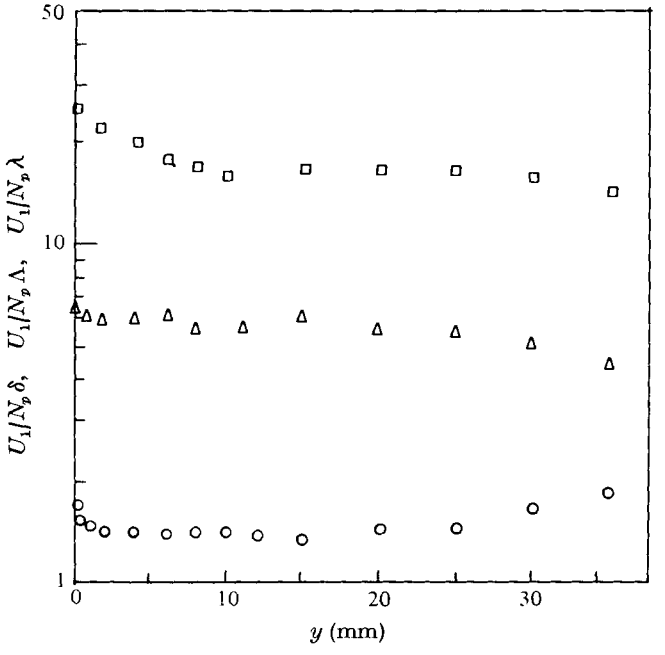

FIGURE 14. Scaling of the pulse rate with different length scales across the boundary layer. Flat plate, $R_\theta = 3000$, $\delta = 34$ mm. □, $U_1/N_p\lambda$; △, $U_1/N_p\Lambda$; ○, $U_1/N_p\delta$.

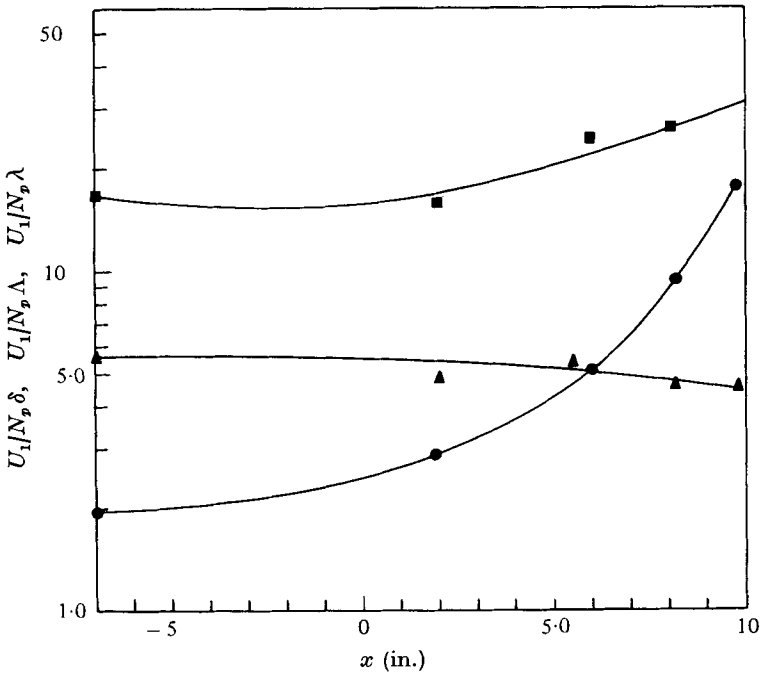

FIGURE 15. Scaling of pulse rate with different length scales. Accelerated flow, $y/\delta = 0{\cdot}5$. Symbols as in figure 13.

the Reynolds number. In boundary-layer flows, the present experiments indicate that the ratio Λ/λ varies between 3 and 5, a result which is appreciably different from that for grid turbulence (figure 5). There seems to be a definite relation between δ, λ and Λ and on account of this all three non-dimensional parameters indicate the same trend. However, a close look at the results suggests that in boundary-layer flows too Λ might be the fundamental length scale that characterizes N_p since $U_1/N_p\,\Lambda$ is nearly equal to 6·0, the value found in grid turbulence. The variations of $U_1/N_p\,\delta$, $U_1/N_p\,\lambda$ and $U_1/N_p\,\Lambda$ across the boundary layer at a Reynolds number R_θ of 3000 are shown in figure 14.

The investigations in the accelerated boundary-layer flow also confirm that N_p scales with the zero-crossing length scale. The values of $U_1/N_p\,\delta$, $U_1/N_p\,\lambda$ and $U_1/N_p\,\Lambda$ for $y/\delta = 0{\cdot}5$ at various stations x during acceleration are plotted in figure 15. In the region $x = -7$ in. to 2 in., where the pressure gradient is not very severe, all three parameters are nearly constant. Beyond $x = 2$ in., $U_1/N_p\,\delta$ rises steeply from 1·8 to 20; a similar trend is evident for $U_1/N_p\,\lambda$, though the increase is less than that in $U_1/N_p\,\delta$. On the other hand, $U_1/N_p\,\Lambda$ is nearly equal to 6·0 at all stations. The above result indicates that the fine-scale structure is governed primarily by the zero-crossing length scale, and that the spatial separation between two high frequency pulses is on average equal to about 6 times the zero-crossing length scale.

In this investigation no attempts were made to relate the high frequency pulses and the zero crossings of the transverse velocity component. However

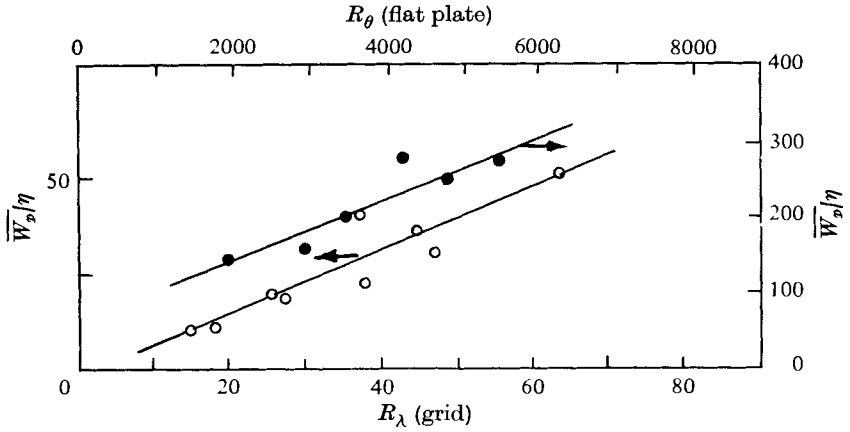

FIGURE 16. Average width of high frequency pulses. ○, grid; ●, flat plate.

some sample measurements made in the early stages of this work showed that the rate of occurrence of the pulses was the same for $u(t)$ as for $v(t)$.

The average width $\overline{W}_p$ of the high frequency pulses, when non-dimensionalized with the Kolmogorov length scale, exhibits a linear relation with the Reynolds numbers R_λ and R_θ respectively in grid turbulence and in boundary-layer flows with zero pressure gradient (figure 16). The result obtained in free turbulent flows by Kuo & Corrsin (1971) using their criterion for fine-scale structure shows an entirely different trend; the width of the fine-scale structure initially decreases with increasing R_λ up to $R_\lambda = 350$ and remains a constant thereafter at a value of 18η. The discrepancy between the two results is somewhat unexpected and could be due to the different procedures adopted in the two experiments for extracting the fine-scale structure. As already pointed out, Kuo & Corrsin used $f_m = N_K$, the Kolmogorov frequency, which lies at the tail end of the dissipation spectrum (figure 2), whereas the present authors have used a frequency f_s which is closer to the maximum dissipation region. f_s is found to be nearly half to one-third of N_K. For example, in the case of the grid flow with a 1·20 in. mesh, for the three different velocities the values of f_s were 1·5 kHz, 2 kHz and 3 kHz, while the corresponding values of N_K were 3 kHz, 4·6 kHz and 8 kHz. Kuo & Corrsin's results represent fine-scale structure in the universal equilibrium range, where the small eddies have practically lost their individual identity and become isotropic, whereas the present investigation deals with eddies which contribute significantly to dissipation but are far away from the Kolmogorov scale.

The coincidence between the occurrence of high frequency pulses and positive runs of u near the wall is consistent with the observations made visually by Corino & Brodkey (1969) and with the more detailed investigations by Brodkey *et al.* (1974) on the cyclic nature of events occurring near the wall. They noticed three types of major event, namely deceleration, ejection and inrush. During ejection, the locally decelerated flow is thrown outwards in the form of small jets, and on account of the instability of the jet flow, one can expect the outward-moving jets to contain high frequency energy. The occurrence of high frequency pulses during positive runs of u seems to represent a combination of the

acceleration and ejection processes. The strong correlation noticed between streamwise vorticity and the negative part of u at the edge of the sublayer by Willmarth & Lu (1972) supports the present observation. The constancy of N_p with y from $y_* = 50$ up to the interface region in the boundary layer (figure 7) suggests the possibility that the vortex filaments thrown out from the sublayer during ejection persist right across the boundary layer. This process can be considered as an important basic mechanism in turbulent boundary-layer flows that is responsible for turbulent transport controlling mass, momentum and heat transfer.

The other observation, namely that high frequency pulses in the outer part of the boundary layer are found to occur simultaneously with u_- and v_+, suggests either of two flow models. The first is that the vortex filaments thrown out during ejection re-enter the flow, forming a cyclic process. The second one is that the vortex filaments ejected from the wall region are dissipated as they move outside and fresh vortex filaments created in the interface region. Since no correspondence could be detected between the high frequency pulses and the negative or positive part of turbulence signals in the central region of the boundary layer, a definite choice between these two models could not be made.

The measurements of the four components of the Reynolds stress (figure 9) indicate that the u_-v_+ and u_+v_- components are the main contributors, with maximum values near the wall. Both these components decrease in strength with distance from the wall. One can understand that the jet-like ejections lose their strength as they penetrate the flow. Similarly, the flow required by continuity to replace fluid ejected from near the wall has a maximum in the wall region. The whole process seems to be cyclic in nature, the outer flow most probably interacting with the inner flow in a nonlinear way, with the re-entering inrush flow responsible for triggering the turbulent bursts at the wall observed by Kline *et al.*

In this context the authors would like to point out that the fine-scale structures of turbulence in the sense used in this paper are not necessarily those which carry most of the large instantaneous shear stress. Detailed investigations made recently by Sabot & Comte-Bellot (1976) (also see Falco 1974) indicate that the large-scale 'bursty' nature of the flow is responsible for the transport of the shear stress. It is possible that the fine-scale structures are embedded in the bursts, forming the high frequency parts of them.

In the accelerated boundary layer, in the initial region from $x = -7$ in. to $x = 2$ in. the synchronization of the u runs with high frequency pulses is the same as in a flat-plate boundary layer (figure 10). However, in the region of higher acceleration downstream, the coincidence coefficient between the two signals slowly decreases and no special preference (50 % coincidence) is found at $x = 8$ in. The lower coincidence of pulses and a positive u signal in the wall region suggests that the flow structure has undergone some definite changes; the cyclic process has presumably been disturbed. Even though one cannot rule out completely the production of high frequency energy in the wall region, most of the pulses recorded at any station downstream in the highly accelerated zone seem to be the remnants of the convected vortex filaments produced upstream.

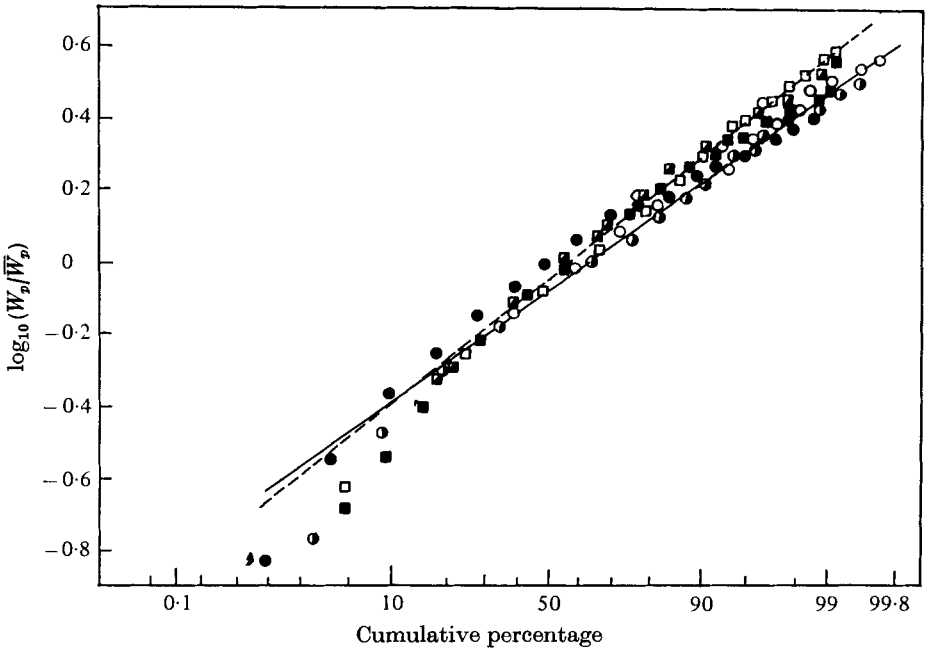

FIGURE 17. Probability distribution of pulse width. $y/\delta = 0{\cdot}4$, standard deviation = 0·25. Flat plate: ○, $R_\theta = 5500$; ◑, $R_\theta = 4200$; ●, $R_\theta = 1900$. Grid: □, $M = 1{\cdot}20$ in., $U_1 = 38{\cdot}6$ ft/s, $R_\lambda = 44{\cdot}5$; ■, $M = 0{\cdot}50$ in., $U_1 = 61{\cdot}7$ ft/s, $R_\lambda = 47{\cdot}2$; ■, $M = 0{\cdot}25$ in., $U_1 = 40{\cdot}5$ ft/s, $R_\lambda = 25{\cdot}5$.

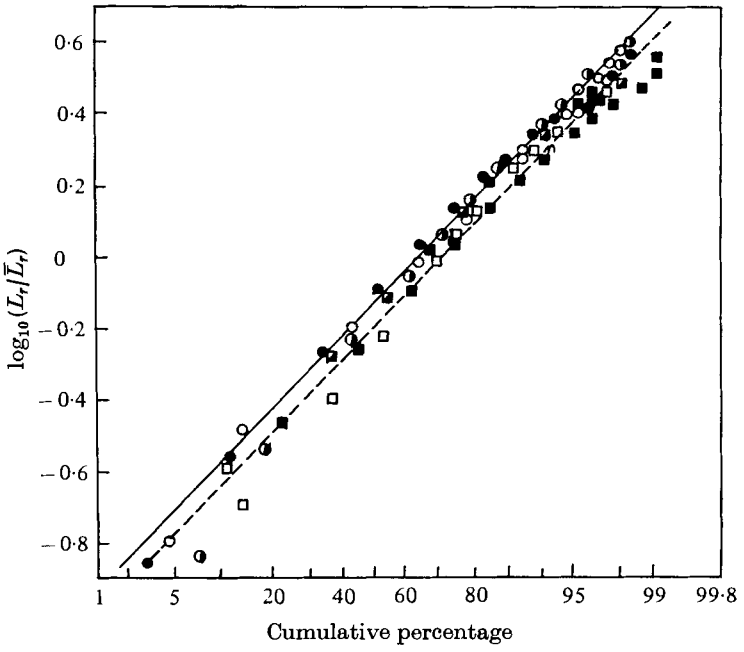

FIGURE 18. Probability distribution of the length of runs. Standard deviation = 0·35. Flat plate: ○, $y = 0{\cdot}3$ mm; ◑, $y = 10$ mm; ●, $y = 35$ mm. Grid: □, $M = 1{\cdot}20$ in., $U = 28$ ft/s, $R_\lambda = 37{\cdot}9$; ◪, $M = 0{\cdot}50$ in., $U = 40{\cdot}5$ ft/s, $R_\lambda = 27{\cdot}4$; ■, $M = 1{\cdot}20$ in., $U = 38{\cdot}6$ ft/s, $R_\lambda = 44{\cdot}5$.

This idea is supported to some extent by the observation that all the turbulence quantities, namely $\overline{u^2}$, $\overline{v^2}$ and $\overline{uv}$, are almost constant along streamlines in the favourable-pressure-gradient region. In addition, the cessation of bursts reported by Schraub & Kline (1965) in favourable-pressure-gradient flows and the poor correlation between runs and pulses in the wall region might indicate the same phenomenon. More detailed investigations in the wall region during acceleration must be made to confirm this trend.

The probability distributions of the width of the fine-scale structure for the flat-plate boundary layer as well as for grid turbulence are plotted in figure 17. Similarly, the lengths L_r of the u runs for both cases are shown in figure 18. Both quantities show a nearly lognormal distribution. In addition, even though the slopes of the distributions of W_p are different from those of L_r, individually these quantities seem to have the same slope irrespective of the type of flow, indicating some kind of universality. Rao *et al.* (1971) have already shown that the time interval between two high frequency pulses is also lognormally distributed. Hence on the whole one can conclude that the vortex tubes are lognormally distributed in width as well as in spacing in turbulent flows in general.

6. Conclusions

In this paper some properties of the fine-scale structure of turbulence have been investigated experimentally. 'Fine-scale structure' means, in the authors' opinion, small eddies which are different from energy-containing eddies. The experiments of Rao *et al.* (1971) as well as the results of the present investigation have demonstrated that, above a certain filter frequency f_s, the rate of occurrence of high frequency pulses is independent of the filter frequency. This result is significant as it provides a logical demarcation frequency for small eddies. A closer examination of the energy and dissipation spectra indicates that this frequency f_s is slightly higher than the frequency corresponding to maximum dissipation, but nearly one-third to one-half of the Kolmogorov frequency. Motions at and beyond the frequency f_s are termed 'fine-scale structure' in the present paper.

The above paragraph is included here mainly to make the definition of the fine-scale structure of turbulence used in this report clear since this terminology has been used with slightly different criteria by different investigators in the past few years.

Experiments were conducted in grid turbulence, in boundary layers with a zero pressure gradient as well as in a boundary layer with a favourable pressure gradient leading to relaminarization. The conclusions arrived at are as follows.

(i) For all three flows the rate of occurrence N_p of high frequency pulses was found to scale with the zero-crossing length scale $\Lambda = U_1/\pi N_z$, where N_z is the rate of zero crossing of the u signal and U_1 is the free-stream velocity. $U_1/N_p\Lambda$ was found to be almost constant at nearly 6·0 at all Reynolds numbers irrespective of the flow.

(ii) In grid turbulence Λ/λ was found to be nearly unity whereas in boundary-layer flows Λ/λ varied between 3 and 5, if U_1 was used to define Λ.

(iii) The values of the pulse rate N_p determined by using the technique described in § 2 were found to be nearly equal to half the rate of zero crossing of the unprocessed signal in all three flows.

(iv) The width of the high frequency pulses indicated a nearly lognormal distribution, the ratio $\overline{W}_p/\eta$ increasing linearly with Reynolds number.

(v) The length of the runs also exhibited a nearly lognormal distribution.

(vi) The coincidence noticed between the sign of the u fluctuation and high frequency pulses in flat-plate boundary layers almost disappeared during high acceleration.

All the above results lead to the basic conclusion that the fine-scale structure consists of vortex filaments which are convected by the fluid at a velocity proportional to the mean free-stream velocity and have an average spacing of about 6 times the zero-crossing length scale. The width of the vortex filaments is $a\eta$, where η is the Kolmogorov microscale and a varies linearly with Reynolds number over the range covered here. The zero-crossing length scale seems to play a fundamental role in turbulent flows.

REFERENCES

ANTONIA, R. A. 1973 *Phys. Fluids*, **16**, 1198.

BADRI NARAYANAN, M. A. & RAMJEE, V. 1969 *J. Fluid Mech.* **35**, 225.

BADRI NARAYANAN, M. A., RAJAGOPALAN, S. & NARASIMHA, R. 1974 *Dept. Aero. Engng, Indian Inst. Sci. Rep.* 74 FM 15.

BADRI NARAYANAN, M. A., RAO, K. N. & NARASIMHA, R. 1971 *Proc. 4th Austr. Conf. Hydraul. Fluid Mech.*, p. 73.

BATCHELOR, G. K. & TOWNSEND, A. A. 1948 *Proc. Roy. Soc.* A **193**, 539.

BATCHELOR, G. K. & TOWNSEND, A. A. 1949 *Proc. Roy. Soc.* A **199**, 238.

BLACKWELDER, R. F. & KOVASZNAY, L. S. G. 1970 *Interim Tech. Rep., Dept. Mech., John Hopkins Univ.*

BRODKEY, R. S., WALLACE, J. M. & ECKELMANN, H. 1974 *J. Fluid Mech.* **63**, 209.

COLES, D. 1962 *Rand Corp. Rep.* R-403-PR.

CORINO, E. R. & BRODKEY, R. S. 1969 *J. Fluid Mech.* **37**, 1.

CORRSIN, S. 1962 *Phys. Fluids*, **5**, 1301.

FALCO, R. E. 1974 *A.I.A.A. 12th Aero. Sci. Meeting, Washington*, paper 74–79.

GRANT, H. C., STEWART, R. W. & MOILLIET, A. 1962 *J. Fluid Mech.* **12**, 241.

KENNEDY, D. A. & CORRSIN, S. 1961 *J. Fluid Mech.* **10**, 366.

KLEBANOFF, P. S. 1954 *N.A.C.A. Tech. Note*, no. 3178.

KLINE, S. J., REYNOLDS, W. C., SCHRAUB, F. A. & RUNSTADLER, P. W. 1967 *J. Fluid Mech.* **30**, 741.

KOLMOGOROV, A. N. 1941 *C.R. Acad. Sci. (Doklady) U.S.S.R.* **30**, 301.

KUO, A. S. & CORRSIN, S. 1971 *J. Fluid Mech.* **50**, 285.

KUO, A. S. & CORRSIN, S. 1972 *J. Fluid Mech.* **56**, 447.

LAUFER, J. 1951 *N.A.C.A. Tech. Note*, no. 1174.

LIEPMANN, H. W., LAUFER, J. & LIEPMANN, K. 1951 *N.A.C.A. Tech. Note*, no. 2473.

LU, S. S. & WILLMARTH, W. W. 1973 *J. Fluid Mech.* **60**, 481.

RAO, K. N., NARASIMHA, R. & BADRI NARAYANAN, M. A. 1971 *J. Fluid Mech.* **48**, 339.

SABOT, J. & COMTE-BELLOT, G. 1976 *J. Fluid Mech.* **74**, 767–796.

SANDBORN, V. A. 1959 *J. Fluid Mech.* **6**, 221.

SCHRAUB, F. A. & KLINE, S. J. 1965 *Dept. Mech. Engng, Stanford Univ. Rep.* MD-12.

TENNEKES, H. 1968 *Phys. Fluids*, **11**, 669.

TOWNSEND, A. A. 1956 *The Structure of Turbulent Shear Flow*. Cambridge University Press.

WILLMARTH, W. W. & LU, S. S. 1972 *J. Fluid Mech.* **55**, 65.

WYNGAARD, J. C. & TENNEKES, H. 1970 *Phys. Fluids*, **13**, 1962.